TECHNICAL MEMORANDUM

836

Weakly coupled ocean–atmosphere data assimilation in the ECMWF NWP system

Philip Browne, Patricia de Rosnay, Hao Zuo, Andrew Bennett, Andrew Dawson

Research Department

To be submitted to Remote Sensing

December 18, 2018

European Centre for Medium-Range Weather Forecasts
Europäisches Zentrum für mittelfristige Wettervorhersage
Centre européen pour les prévisions météorologiques à moyen terme

Series: ECMWF Technical Memoranda

A full list of ECMWF Publications can be found on our web site under:
http://www.ecmwf.int/en/research/publications

Contact: library@ecmwf.int

European Centre for Medium-Range Weather Forecasts
Shinfield Park, Reading, RG2 9AX, England

Abstract

Numerical weather prediction models are including an increasing number of components of the Earth system. In particular, every forecast now issued by the European Centre for Medium-range Weather Forecasts (ECMWF) runs with a 3D ocean model and a sea ice model below the atmosphere. Initialisation of different components using different methods and on different timescales can lead to inconsistencies when they are combined in the full system. Historically, the methods for initialising the ocean and the atmosphere have typically been developed separately. This paper describes an approach for combining the existing ocean and atmospheric analyses into what we categorise as a weakly coupled assimilation scheme. Here we show the performance improvements for the atmosphere by having a weakly coupled ocean–atmosphere assimilation system compared to an uncoupled system. Using numerical weather prediction diagnostics we show that forecast errors are decreased compared to forecasts initialised from an uncoupled analysis. Further, a detailed investigation into spatial coverage of sea ice concentration in the Baltic sea shows much more realistic structure given by the weakly coupled analysis. By introducing the weakly coupled ocean–atmosphere analysis, the ocean analysis becomes a critical part of the numerical weather prediction system and provides a platform from which to build ever stronger forms of analysis coupling.

1 Introduction

As of June 2018, the European Centre for Medium-range Weather Forecasts (ECMWF) has a coupled forecasting system for all timescales in that every forecast from the high resolution 10 day forecasts, the ensemble forecasts, the monthly forecasts to the seasonal prediction system runs an Earth system model. Specifically this means that there is a 3-dimensional ocean model and a sea ice model that runs coupled to the atmosphere, wave, and land surface components. Such a multi-component Earth system model needs initialisation of each of its components, and this manuscript is concerned with how the ocean and atmosphere are initialised together for the purposes of numerical weather prediction.

In order to advance numerical weather prediction, ECMWF is developing its modelling and its data assimilation towards an Earth system approach [ECMWF, 2016]. When forecasts of medium-range to longer-range are the focus, components of the Earth system that are typically slower than the atmosphere become more important. This is both in terms of their presence in the model and an accurate specification of their initial conditions [Bauer et al., 2015]. Such components include the ocean and sea ice, but also the land surface, waves, aerosols, and how they interact with each other and the atmosphere [Maclachlan et al., 2015]. Figure 1 represents the various components present in the system.

The land surface and waves are fully established components of the ECMWF systems. Aerosols are treated separately within the Integrated Forecasting System (IFS) as part of the Copernicus Atmosphere Monitoring Service (CAMS). The ocean has been used in the IFS for seasonal applications since 1997 [Stockdale et al., 1998], for monthly forecast since 2002 [Vitart, 2004] and in the Ensemble Forecasts (ENS) from the initial time step since 2013 [Balmaseda et al., 2013, Bauer and Richardson, 2014]. In late 2016 an interactive sea ice model was added to the ENS. Only now are these components starting to interact with the atmospheric analyses.

In order to make the most of the Earth system approach in a forecast, the components should be somehow consistent with one another. If the different components are not internally consistent they are sometimes referred to as *unbalanced*. This lack of balance can lead to fast adjustments in the system in the initial stages of the forecast in a phenomenon known as *initialisation shock*. Initialisation shock can be reduced by initialising the various components together via coupled data assimilation [Mulholland et al., 2015].

Much of the literature on coupled assimilation has focused on initialisation of forecasts for seasonal to

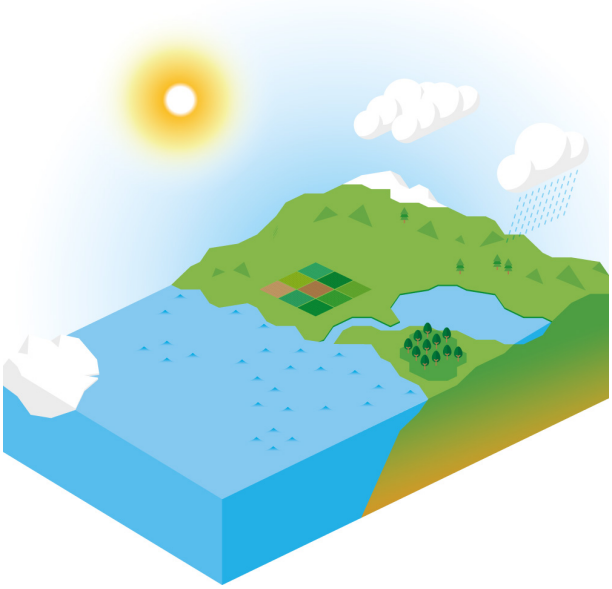

Figure 1: Components of ECMWF's IFS Earth System. Along with the atmosphere, there are the ocean, wave, sea ice, land surface, and lake models.

decadal timescales. For example the Japan Agency for Marine-Earth Science and Technology (JAMSTEC) have a fully coupled 4D-Var system used for experimental seasonal and decadal predictions [Sugiura et al., 2008, Masuda et al., 2015, Mochizuki et al., 2016]. The National Oceanic and Atmospheric Administration Geophysical Fluid Dynamics Laboratory (NOAA/GFDL) have a coupled assimilation system based on the ensemble Kalman filter (specifically the ensemble adjustment Kalman filter) to initialise decadal predictions [Yang et al., 2013, Zhang et al., 2014]. The NOAA National Centers for Environmental Prediction (NOAA/NCEP) have a coupled assimilation system [Saha et al., 2014] for subseasonal and seasonal predictions, as well as reanalysis [Saha et al., 2010]. A prototype system was built in March 2016 in the Japan Meteorological Agency Meteorological Research Institute (JMA/MRI), designed to replace the ocean-only observation assimilation approach. The atmosphere component is updated every 6-hours by 4D-Var with a TL159L100 uncoupled inner-loop model, while the ocean component runs on a 10-day cycle using 3D-Var with an incremental analysis update. Experimentation with this system for coupled reanalysis and NWP is underway [Penny et al., 2017].

The U.S. Naval Research Laboratory (NRL) has a different focus to most centres, running a coupled model with most resources dedicated to the ocean component. Their global coupled model goes up to an ocean resolution of $1/25^\circ$ and is initialised by separate assimilation systems. In the near future they plan to implement the interface solver of Frolov et al. [2016] to allow more coupling within the analysis.

Environment and Climate Change Canada (ECCC) have recently begun producing their global deterministic NWP forecasts using a coupled ocean–atmosphere model. This model is currently initialised separately in each of its components. The UK Met Office have a system to initialise global coupled NWP forecasts where the background for each component in a 6 hour assimilation window comes from the coupled model [Lea et al., 2015], although this is not yet operational.

Under the ERA-CLIM2 project ECMWF has piloted techniques for coupled ocean–atmosphere data assimilation that were applied in the context of reanalysis [Laloyaux et al., 2016, Schepers et al., 2018]. These are the Coupled European Reanalysis of the 20th century (CERA-20C) and the CERA-SAT reanalysis using the modern day satellite observation system. The assimilation method developed for CERA

involved "outer-loop" coupling within the 4D-Var algorithm of the atmosphere and the ocean. This method has a high level of coupling in the analysis, which as Figure 2 shows, can mean that the whole NWP system can be degraded by model biases in the ocean component of the coupled model.

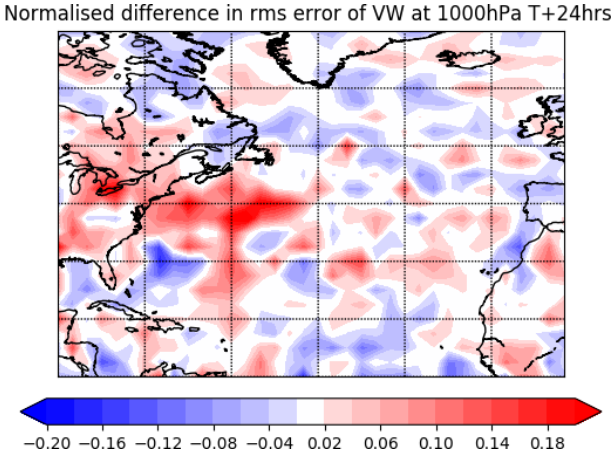

Figure 2: Impact of first implementation of outer loop coupling (quasi strongly coupled data assimilation) on high resolution global NWP. The presence of model bias in the western boundary currents of the ocean shows itself as degradations (red) to the 24 hour forecast scores of vector winds at 1000hPa. Results are obtained from IFS cycle 45R1 at a resolution of 25km (TCo399) with a 0.25° ocean, based on global outer loop coupling over the period 2017-06-01–2017-07-02.

As the first steps into coupled ocean–atmosphere data assimilation for NWP at ECMWF we have chosen to adopt a weaker form of coupled assimilation than in the CERA system.

Following a World Meteorological Organisation (WMO) meeting on coupled assimilation, Penny et al. [2017] defined *weakly* and *strongly* coupled data assimilation (and variations thereof). Their definitions were as follows:

- "Quasi Weakly Coupled DA (QWCDA) assimilation is applied independently to each of a subset of components of the coupled model. The result may be used to initialize a coupled forecast."
- "Weakly Coupled DA (WCDA): assimilation is applied to each of the components of the coupled model independently, while interaction between the components is provided by the coupled forecasting system."
- "Quasi Strongly Coupled DA (QSCDA): observations are assimilated from a subset of components of the coupled system. The observations are permitted to influence other components during the analysis phase, but the coupled system is not necessarily treated as a single integrated system at all stages of the process."
- "Strongly Coupled DA (SCDA): assimilation is applied to the full Earth system state simultaneously, treating the coupled system as one single integrated system. In most modern DA systems this would require a cross-domain error covariance matrix be defined."

Hence QWCDA might be thought of as uncoupled assimilation to initialize a coupled model. Observations in one component never influence the analysis of the other component. In WCDA, an observation of one component is not able to directly influence the analysis of the other component in the valid assimilation window. However, as a coupled forecast is used, the observational information gets propagated

to the background used for subsequent analysis cycles, hence there is a lag by which observations can influence different components. The CERA system falls under the QSCDA category, where observations from each component can influence the analysis of the other within a single analysis window. SCDA is simply treating a coupled system as a multivariate assimilation problem and no special terminology or mathematical analysis is necessary.

In this paper we introduce a form of weakly coupled data assimilation which allows for the different timescales in the ocean and atmospheric analysis windows. The atmosphere and the ocean are coupled implicitly at a frequency of 24 hours, determined by the frequency of the slowest component to update.

The remainder of this paper is organised as follows. In Section 2 we describe the various components of the Integrated Forecasting System and describe both uncoupled and weakly coupled ocean–atmosphere assimilation strategies. The experimental design is described in Section 3. Section 4 shows and discusses the experimental results, and gives a detailed examination of local impacts to sea ice. Finally in Section 5 we look to the future developments of the weakly coupled data assimilation system at ECMWF.

2 IFS

The ECMWF Integrated Forecasting System consists of multiple components. The main component for it all is the upper atmospheric analysis. The dynamical model which propagates the analysis from one cycle to the next contains a limited number of components. They are the *atmospheric model* [ECMWF, 2017a,b], the *land* model [Balsamo et al., 2009], the *lake* model [Dutra et al., 2009], and the *wave* model [ECMWF, 2017c]. The atmosphere is represented on a 3D reduced Gaussian grid and its analysis is found by using 4-Dimensional Variational data assimilation (4D-Var) in incremental form. A number of outer loops are used and the minimisation is performed at increasingly high resolution. The number of outer loops and resolution of the inner loops is dependent on the resolution of the nonlinear model. The land data assimilation component is weakly coupled to the atmosphere. They share the same model to produce the first guess, and the state of the land surface and the state of the atmosphere are modified separately [de Rosnay et al., 2014]. Subsequent forecasts are initialised using the latest analysis of the atmosphere and the land surface. This is archetypal *weakly coupled* assimilation as defined previously. Currently the land surface has various components. The *snow analysis* is performed using a 2D-OI, as is the *soil temperature* analysis. *Soil moisture* is analysed using a Simplified Extended Kalman Filter (SEKF). Similarly to the land, the *wave analysis* is weakly coupled to the atmosphere. However, the first guess used for the wave analysis is not the same first guess that is used for the atmosphere. The first guess is the nonlinear trajectory of one of the outer loops of the atmospheric 4D-Var. Currently the final trajectory is used. This means that, in a given cycle, observations of the atmosphere will influence the wave analysis in that given cycle. The opposite is not true – wave observations will not modify the atmospheric state during that cycle. These observations will only modify the atmospheric state at the subsequent cycles due to the interactions in the forecasts that cycle the analysis.

The model that cycles the analysis does not contain a dynamical ocean model or sea ice model. For the purposes of this paper we say it is *uncoupled*, referring to ocean–atmosphere interactions. The lower boundary of the atmosphere needs to be supplied; the sea-surface temperature (SST) field and sea ice concentration (CI) field is required.

Observations

Over 40 million observations are processed and used daily with the vast majority of these coming from satellites. These include polar orbiting and geostationary, infrared and microwave imagers, scatterometers, altimeters, and GPS radio occultations [English et al., 2013]. In addition to the satellite observations there are in situ observations used from aircraft, radiosondes and dropsondes, as well as observations from ships, buoys, land based stations and radar [Haiden et al., 2018].

For the sea surface L4 gridded products are used to give global coverage of sea-surface temperatures and sea ice concentrations. The L4 product used is the Operational Sea Surface Temperature and Sea Ice Analysis (OSTIA) [Donlon et al., 2012], a 0.05° resolution dataset that is solely observation based. For SST OSTIA combines satellite data from the Group for High Resolution Sea Surface Temperature (GHRSST) and in-situ observations to produce a daily analysed field of foundation sea-surface temperature. Sea ice concentration fields in OSTIA are derived from the EUMETSAT Ocean Sea Ice Satellite Application Facility (OSI SAF) L3 OSI-401-b observations of sea ice concentration. Lake ice concentration observations that are outside of the domain of OSI-401-b are taken from an NCEP sea ice concentration product.

4D-Var, HRES and the EDA

The above observations are assimilated with the 4D-Var methodology (see e.g. Rabier et al. [2000]) that uses, amongst other details, hybrid-B and a weak constraint term. A single high resolution (HRES) analysis and forecast is produced. The flow dependent component of the background error covariance matrix B comes from an Ensemble of Data Assimilations (EDA) [Bonavita et al., 2012] that solves similar 4D-Var problems but at a lower resolution and with stochastically perturbed observations. The EDA currently runs with 25 members. The HRES analysis is performed twice daily over a 12 hour analysis window from 2100Z (0900Z) to 0900Z (2100Z). The 4D-Var is solved in incremental form with 3 outer loops, such that each inner loop minimisation is performed on a lower resolution grid. From each analysis a 10 day coupled ocean–atmosphere forecast is produced. For more details on the configuration see Haseler [2004].

OCEAN5

OCEAN5 is a reanalysis-analysis system with 2 streams - behind real-time and real-time. The 3 dimensional ocean Nucleus for European Modelling of the Ocean (NEMO) model and the Louvain-la-Neuve 2 (LIM2) sea ice model are coupled and used as the model for within OCEAN5. The OCEAN5 analysis is initialized from a behind real time ocean and sea ice coupled reanalysis, known as ORAS5 [Zuo et al., 2018] (see purple boxes in Figure 3). The variables temperature, salinity, and horizontal currents (T, S, U, V) are analysed using the 3D-Var First Guess at Appropriate Time (FGAT) assimilation technique. The length of the assimilation window varies from 8 to 12 days and is split into two *chunks* (see blue boxes in Figure 3), the first of which is 5 days long. In parallel, a separate minimisation is performed to analyse sea ice concentration using the same 3D-Var FGAT method.

Observations that are assimilated currently are in situ profiles of temperature and salinity, and satellite derived sea level anomaly and sea ice concentration observations. For SST a relaxation is performed towards the OSTIA SST product.

The ocean and sea ice analysis system requires forcing fields in the form of a surface wind field, surface

temperature and humidity fields, and surface fluxes. These come from the HRES analysis (and forecast for the final day of the OCEAN5 assimilation window). The surface fluxes consist of downward solar radiation, thermal radiation downwards, total precipitation, and snowfall. From the wave model the ocean requires forcing fields of significant wave height, mean wave period, coefficient of drag with waves, ten metre neutral windspeed, normalized energy flux into the ocean, normalized wave stress into the ocean, and Stokes drift. A full description is given in Zuo et al. [2018].

Uncoupled approach/work flow

From the above description, we can see that the HRES system can stand alone. It does not require any information from the OCEAN5 analysis. OCEAN5 on the other hand, requires forcing fields from an atmospheric analysis to operate.

Under this system, observations in the atmosphere will modify the atmospheric state. This change in atmospheric state will lead to a change in the forcing fields by which the ocean analysis is driven. This will lead to a change in the ocean analysis.

Observations of the ocean (unused by OSTIA, such as observations of currents) will not modify the atmospheric state as no information from the ocean model is propagated back to the atmosphere. This system as a whole can be thought of as a *"one way"* coupled assimilation system. The flow of information from the atmosphere to the ocean is depicted in the diagram in Figure 3 as orange arrows.

WCDA

We have seen that the atmospheric analysis requires the provision of an SST field and a sea ice field for use as its lower boundary condition. Similarly the ocean analysis requires a set of atmospheric forcing fields to drive the ocean only analysis.

To form a weakly coupled ocean–atmosphere data assimilation system, fields from the OCEAN5 analysis are used as the lower boundary conditions for the atmospheric analysis over the ocean, rather than taking directly fields from the external OSTIA product. This will mean that observations of the ocean and the sea ice which previously would only influence the ocean analyses will also modify the atmospheric analysis via the lower boundary conditions. The effect is not within a given assimilation cycle, but it is delayed.

Figure 3 shows the information flow between atmosphere and ocean. Consider an atmospheric observation on day 11 (within the highlighted region). This will change the analysis fields of the atmosphere on day 11, which will lead to the forcing fields that drive the ocean to change. Hence this observation will have an effect on the latest ocean analysis valid at the start of day 12 (which in this diagram has a 11 day window from day 1 to day 12).

Now instead consider an ocean or sea ice observation on day 11. This directly changes the ocean/sea ice analysis for that day, but as there is no feedback to the atmosphere until the end of the window, the atmospheric analysis for day 11 is unchanged. The impact of that ocean or sea ice observation is only detected by the atmosphere on day 12, when the updated sea ice analysis is seen as the lower boundary condition for the atmosphere (magenta arrow in Figure 3).

Recall the definition of Weakly Coupled DA (WCDA): assimilation is applied to each of the components of the coupled model independently, while interaction between the components is provided by the

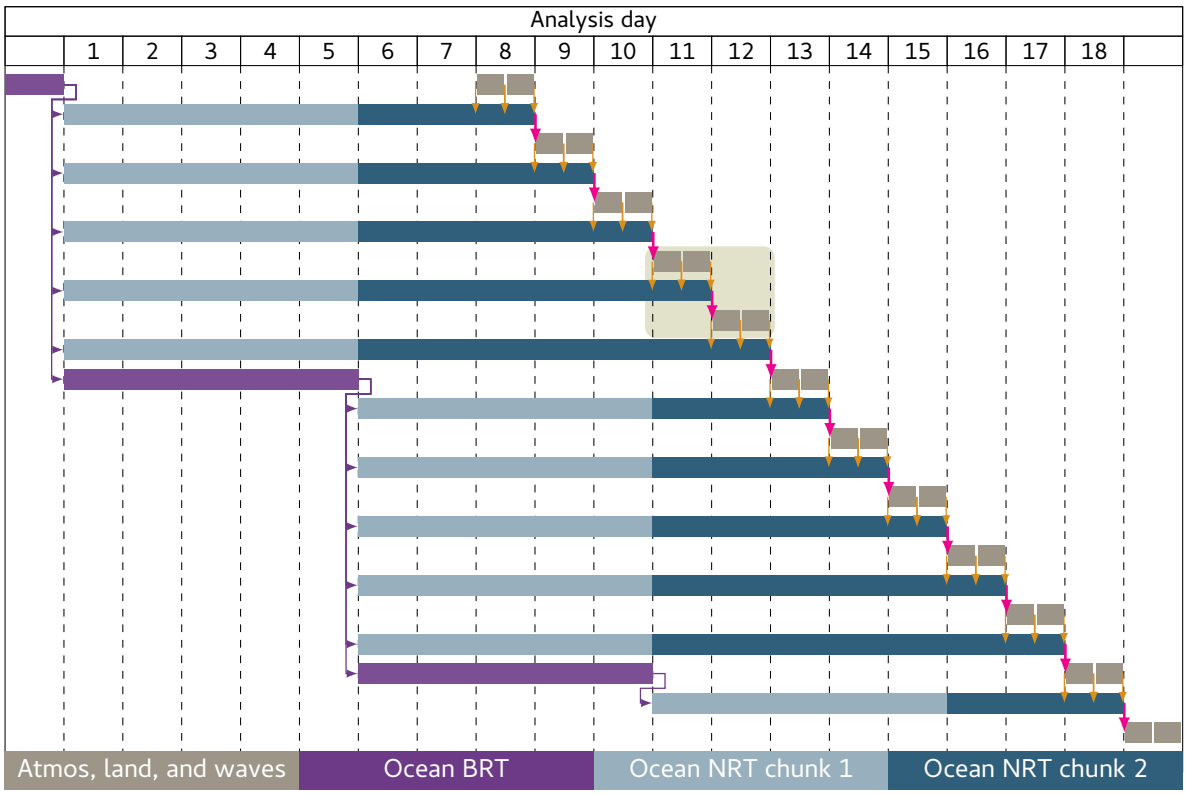

Figure 3: Weakly coupled assimilation system information flow. This is a simplified plot ignoring a 3 hour offset of the systems. Orange arrows show the existing transfer of forcing from the atmosphere to the ocean. Magenta arrows show the addition of taking the OCEAN5 fields and using them as the lower boundary condition for the atmospheric analysis, thus forming the WCDA system. The highlighted region is discussed in an example in the text.

coupled forecasting system. Clearly the assimilation is applied independently to the atmosphere and the ocean/sea ice. Interaction between the components is not provided by a coupled *model* (i.e. a single parallel task on the supercomputer) but by the coupled *forecasting system*. That is, over a 24 hour period the forecasting system passes forcings from the ocean to the atmosphere and lower boundary conditions passed from the ocean/sea ice to the atmosphere. Hence we categorise this as a weakly coupled data assimilation system for the ocean–atmosphere interaction.

Partial coupling

The analysis of SST and sea ice concentration from OCEAN5 may not always be better than the OSTIA product. In particular there are known deficiencies in the OCEAN5 analysis that can lead to degradations in forecast performance. For example in the extratropics the position of western boundary currents such as the Gulf Stream are known to be less accurate in the OCEAN5 analyses compared to OSTIA. Hence for WCDA, as with the model, the flexibility to take ocean fields only over specific regions and not globally has been developed.

The sub-optimality of the ocean analyses are due to a well known model bias in the ocean model which

has been recognised already in the coupled model used to produce the 10 day forecasts [ECMWF, 2014, Mogensen et al, 2019a,b, Keeley et al, 2019]. The solution to this problem has been to use, for the model, a "partial-coupling" approach, where the tendencies, rather than the absolute values, of SST are passed to the atmosphere. The partial coupling is required at latitudes ($> 25°$) where the ocean model is unable to resolve eddies. Partial coupling can be described by the following equations.

$$SST_{\mathrm{IFS}}(t) = SST_{\mathrm{NEMO}}(t) + \alpha(t)\,(SST_{\mathrm{REF}}(0) - SST_{\mathrm{NEMO}}(0)) \tag{1a}$$

where $\alpha(t)$ is a function of lead time with $\alpha(0) = 1$ decreasing to 0 by the end of the forecast. The reference field at initial time, $SST_{\mathrm{REF}}(0)$ is given by

$$SST_{\mathrm{REF}}(0) = \beta SST_{\mathrm{OSTIA}}(0) + (1-\beta) SST_{\mathrm{NEMO}}(0), \tag{1b}$$

where β is spatially varying and is depicted in Figure 4.

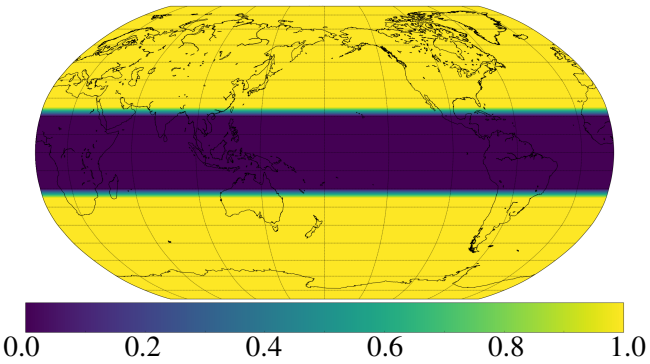

Figure 4: β coefficient from (1b), indicating initial SST is taken from the ocean analysis in the tropics (20S to 20N) and OSTIA in the extratropics. The 5° transition regions can be seen as the bands consisting of intermediate colours.

Equation (1) evaluated at $t = 0$ gives an initial SST field as

$$SST_{\mathrm{IFS}}(0) = \beta SST_{\mathrm{OSTIA}}(0) + (1-\beta) SST_{\mathrm{NEMO}}(0) \tag{2}$$

which is the SST from NEMO in the tropics and the SST from OSTIA in the extratropics. For WCDA we have therefore chosen to align the SST in the analysis with that used to initialise the forecast, i.e. following equation (2).

3 Experimental setup

A set of two experiments are conducted: the first a control which does not use weakly coupled assimilation, and the second an experiment with weakly coupled assimilation. Both experiments are based on IFS cycle 45R1. They run at a 9km global resolution (TCo1279), and both use the same uncoupled atmospheric EDA. The time period of the investigation is from 20170609 to 20180521. From each analysis a *10 day coupled ocean–atmosphere forecast* is produced.

Control - uncoupled assimilation

The initial conditions for the ocean component are taken from an ocean only analysis which takes its forcing fields from the operational HRES system, i.e. the same resolution but atmosphere only and driven

by OSTIA boundary conditions. The atmospheric analysis uses OSTIA SST and CI fields globally as its lower boundary conditions.

Experiment - WCDA

An ocean analysis is run alongside the atmospheric analysis. The sea ice concentration field used for the lower boundary of the atmospheric analysis comes from the ocean analysis. Similarly the sea-surface temperature field comes from the ocean analysis, although this is restricted to the tropics only as described in equation (2) and Figure 4. That is, the SST comes from the ocean analysis between 20S and 20N, OSTIA outside of 25N(S), and a linear interpolation of the two in the 5 degree band from 20N(S) to 25N(S).

The atmospheric analysis is otherwise identical to the control run. Similarly, except for the forcing fields coming from the atmospheric analysis rather than the operational HRES system, the ocean analysis is identical to the ocean analysis used in the control experiment. A comparison of the WCDA experiment and the uncoupled control setup is shown in Figure 5.

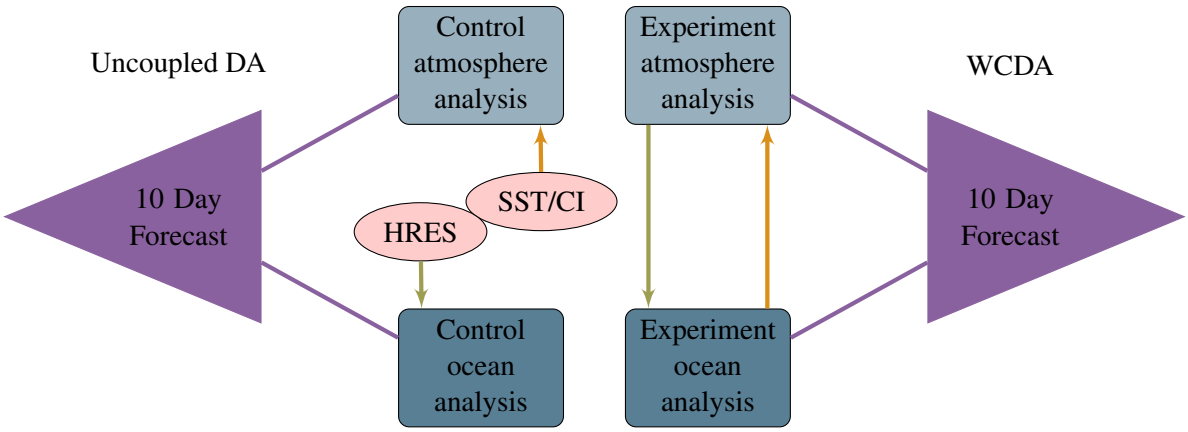

Figure 5: Schematic of experiment design. On the right shows the experiment, with the weakly coupled DA passing information between atmosphere and ocean analyses. On the left shows the control atmospheric analysis getting its SST and CI from the external OSTIA product, and the forcing field for the control ocean analysis coming from the operational HRES system.

4 Results and discussion

For brevity we choose to show normalized differences in RMSE as a measure of forecast errors [Geer, 2016]. Normalised RMSE differences (dRMSE) for an experiment e compared to a control experiment c is defined as

$$\text{dRMSE} = \frac{||\boldsymbol{x}_f^e(T:T+t) - \boldsymbol{x}_a^e(T+t)|| - ||\boldsymbol{x}_f^c(T:T+t) - \boldsymbol{x}_a^c(T+t)||}{||\boldsymbol{x}_f^c(T:T+t) - \boldsymbol{x}_a^c(T+t)||},$$

where $\boldsymbol{x}_f(T:T+t)$ and $\boldsymbol{x}_a(T+t)$ refer to forecasts of length t, and analyses, valid at time $T+t$, and the norm $||\cdot||$ is the root mean square throughout number of samples through time.

Atmospheric performance

Figure 6 shows the impact of WCDA on atmospheric humidity and temperature. There are 3 distinct regions of impact - the tropics and the poles - coming from the separate influences of WCDA through tropical SST and SIC respectively. The areas of hashed shading indicate that the differences in forecast errors are statistically significant. It is clear that the impact from WCDA does not give long range impacts to the upper troposphere or to the spatial regions where WCDA is not active.

In the tropical region of Figure 6 we can see that the impact of the tropical SST is detected from the surface up to around 850hPa, in both temperature and humidity. The hashed shading show that these improvements, indicated by blue colours, are statistically significant. The maps in Figure 7 shows clearly that the improvement from SST is restricted to the latitudinal band for which the WCDA SST is active. Within this band there are variations in how much benefit we get from the WCDA. For instance with temperature at 1000hPa the strongest positive impacts are seen in the Arabian Sea, and the eastern Atlantic and Eastern Pacific (associated with cold tongues).

In the Arabian Sea there is evidence of improvement to other variables, such as to low level winds and significant wave heights (not shown). This indicates that the SST WCDA has improved the position of the summer monsoon which is a known difficult feature to forecast well. The regions of positive impact in the Atlantic and the equatorial Pacific are regions that tend to have high cloud cover. This persistent cloud makes observing the SST from satellites very difficult, and so it may be that the use of the ocean model within the OCEAN5 analysis system is able to effectively fill the observational gap.

In the polar regions we see significant improvements in forecast errors due to the weakly coupled assimilation. Figures 8 and 9 show that the improvements due to sea ice encompasses the entire extent of the sea ice cover, and are not simply confined to the ice edge. The influence of the WCDA SIC extends up to roughly 700hPa (Figure 6). This is further vertically than the impact of SST seen in the tropics. This can be explained by considering Figure 10 that shows the usage of microwave humidity soundings in the southern hemisphere. Such soundings are rejected over sea ice, and hence rejecting more contaminated soundings could lead to a more consistent atmospheric state in these regions. Further area averaged dRMSEs of forecast error are shown in the appendix.

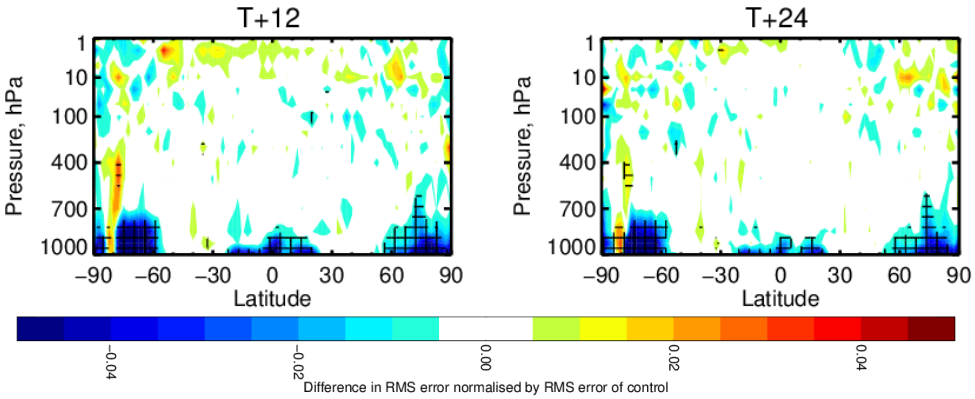

(a) dRMSE of humidity

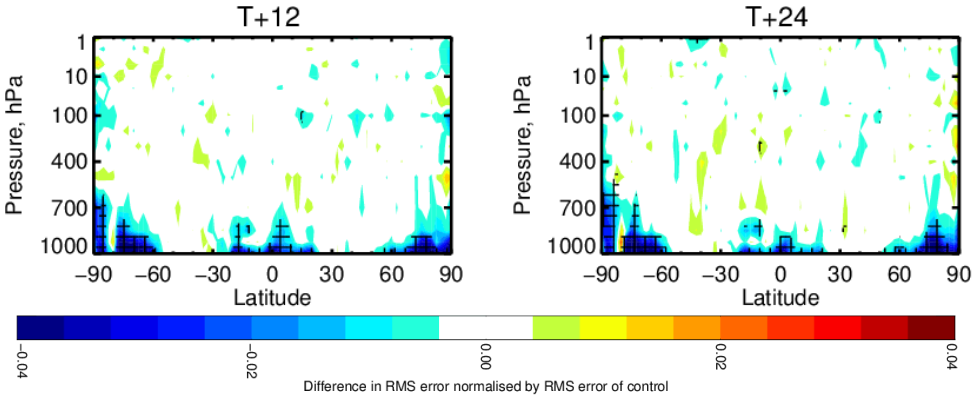

(b) dRMSE of temperature

Figure 6: Latitude–pressure diagram of the normalised difference in RMSE between WCDA and control for humidity (top) and temperature (bottom) forecasts at 12h (left) and 24h (right) lead times, for the period 20170609 to 20180521. Hashed areas indicate statistically significant differences.

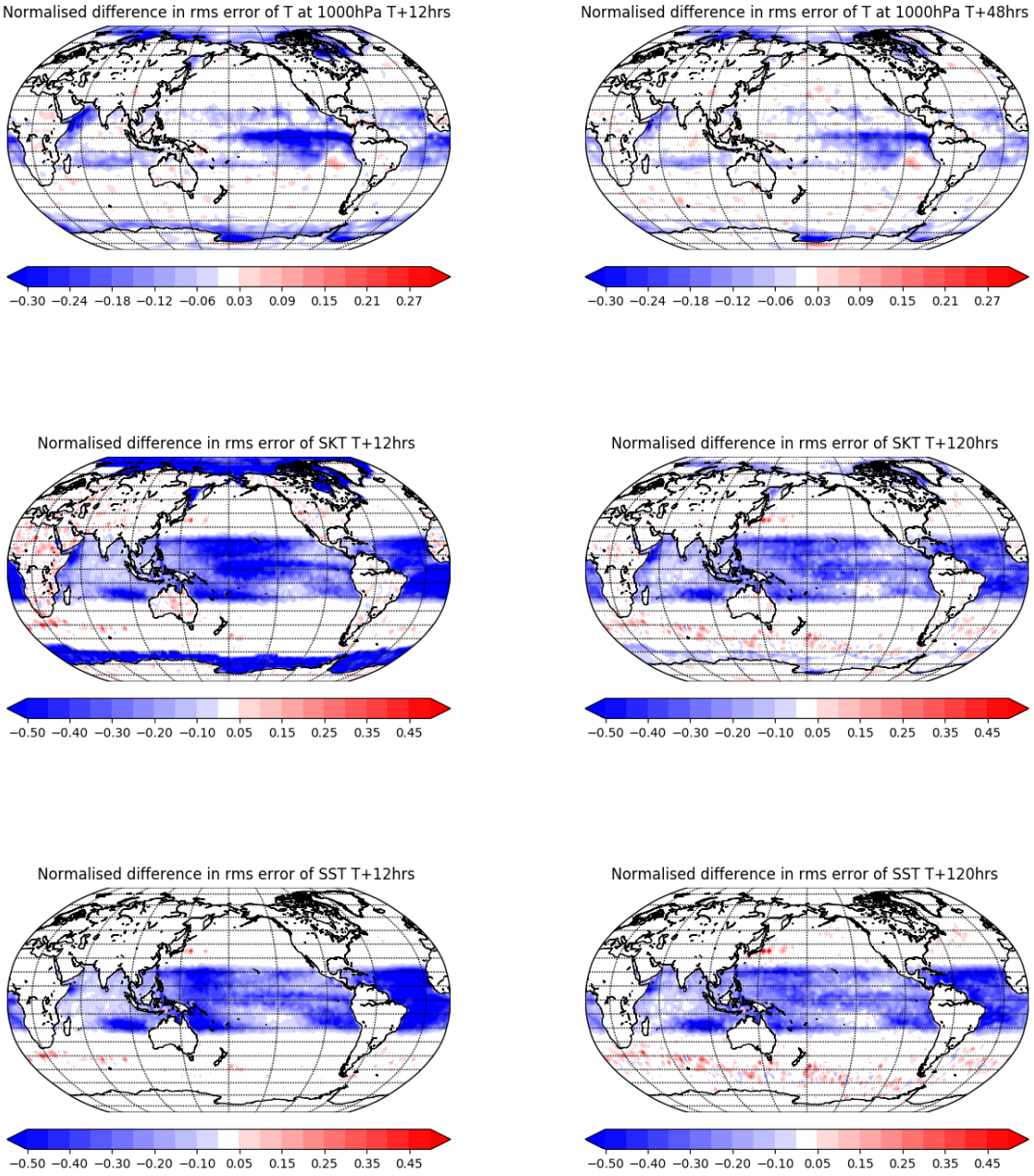

Figure 7: Spatial maps of the normalised difference in RMSE between WCDA and control for temperature at 1000hPa (top), skin temperature (middle), and sea-surface temperature (bottom) forecasts at 12h (left) and 120h (right) lead times (48 hours lead time for temperature at 1000hPa), for the period 20170609 to 20180521.

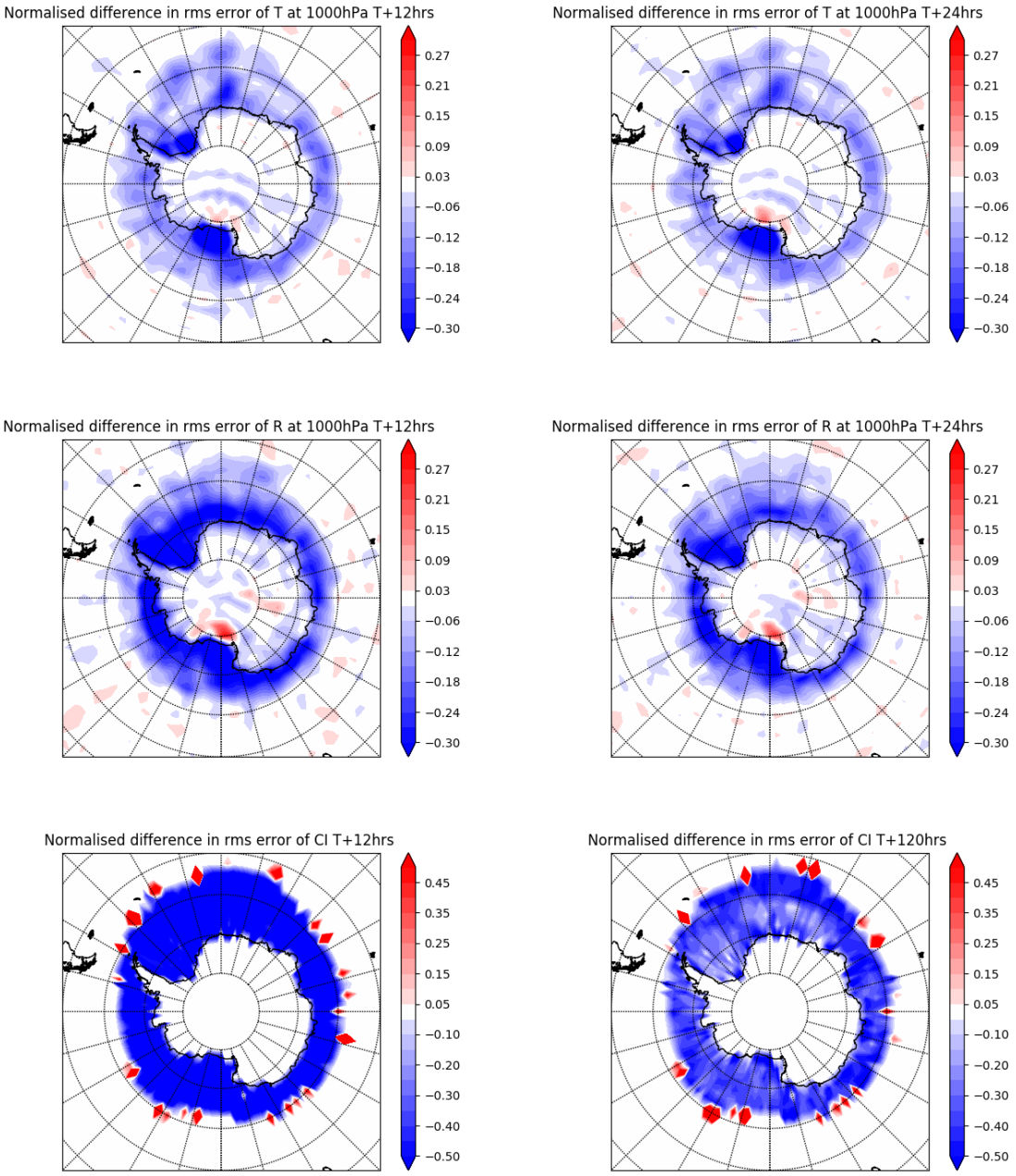

Figure 8: Spatial maps centred on the Antarctic of the normalised difference in RMSE between WCDA and control for 1000hPa temperature (top), 1000hPa humidity (middle), and sea ice concentration (bottom) forecasts at 12h (left) and 24h (right) lead times (120 hours lead time for sea ice concentration), for the period 20170609 to 20180521.

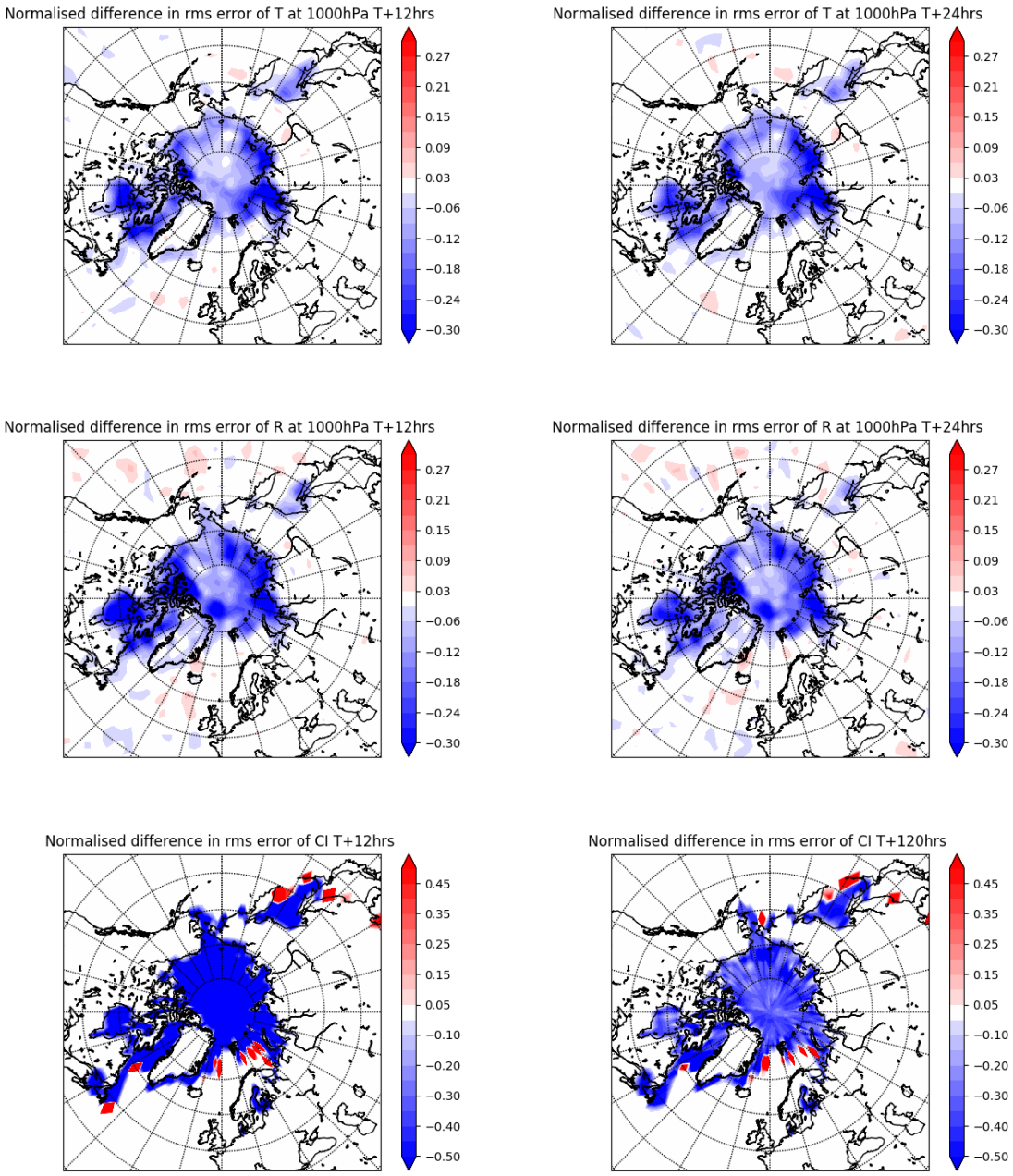

Figure 9: Similar to Figure 8, but focused on the Arctic.

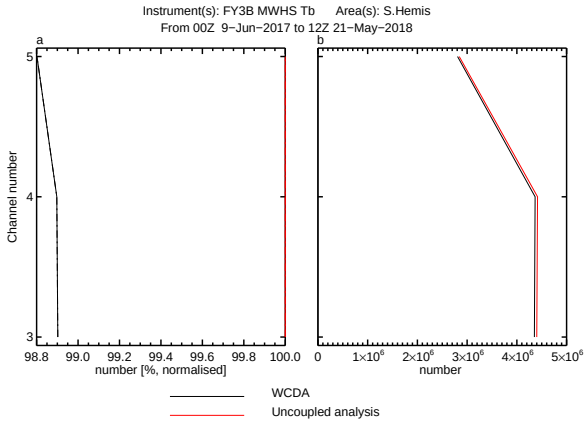

Figure 10: Observation usage of MWHS-1 in the southern hemisphere for the WCDA experiment (black) and the uncoupled control (red).

Ocean performance

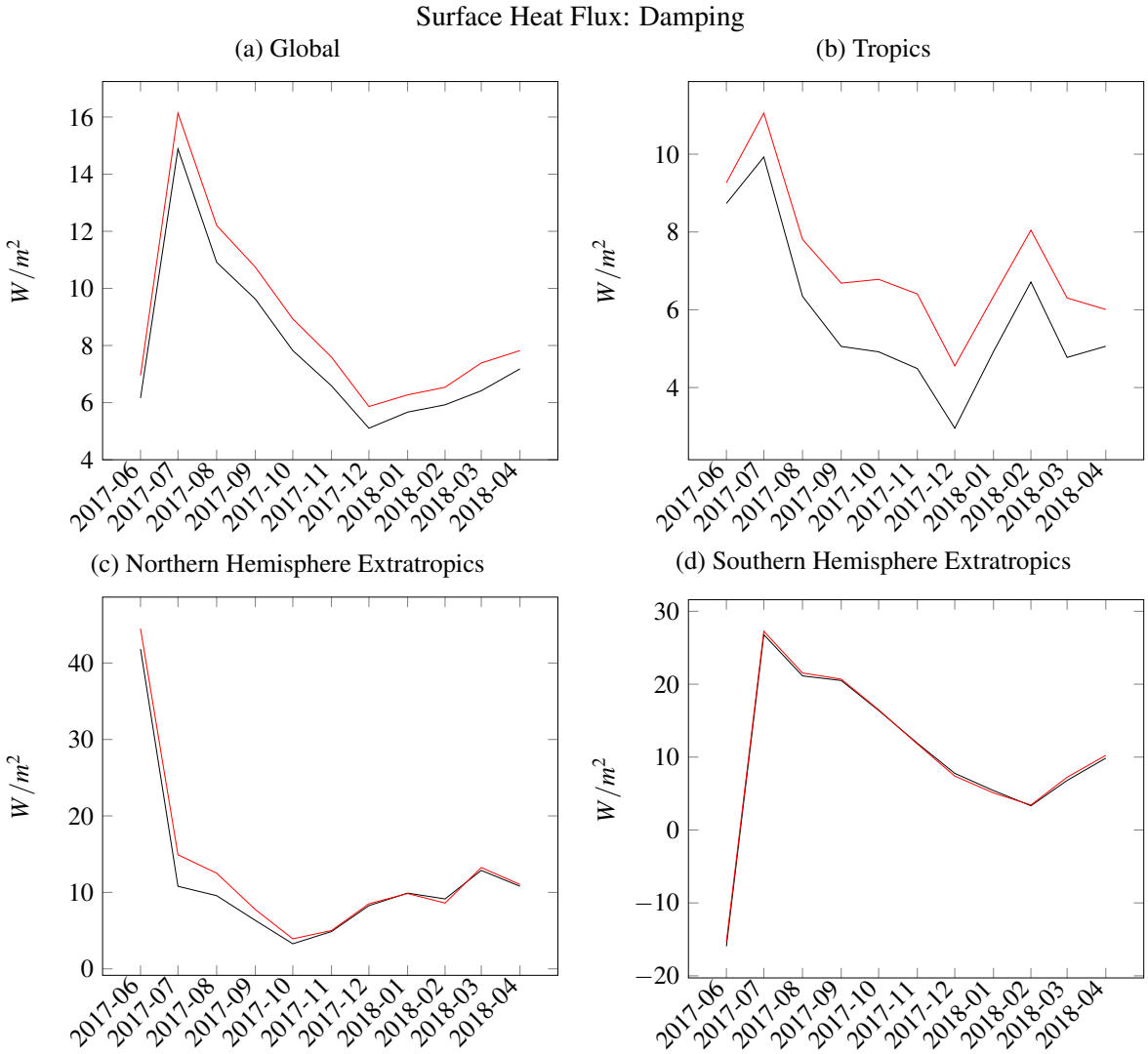

Figure 11: Monthly averaged ocean heat flux correction from the uncoupled analysis (red) and the weakly coupled analysis (black). This is split by region showing global (top left), the tropics (top right), the northern hemisphere extratropics (bottom left) and the southern hemisphere extratropics (bottom right).

Figure 11 shows the area averaged heat flux correction in the ocean analyses. This flux correction represents the strength of the relaxation towards the OSTIA SST product. One can see that the flux correction in the extratropics is broadly similar in both experiments, with only the northern hemisphere extratropics showing a slightly smaller flux correction in July and August in the WCDA experiment. However in the tropics the flux correction is consistently substantially smaller in WCDA than uncoupled. This shows that the SST coupling in the tropics is leading to an SST field that is more consistent than the uncoupled analysis, requiring less corrections. We postulate that this could be due to the improved timeliness of the the SST that the atmospheric component uses (for the uncoupled analysis the OSTIA SST field is only available on the day after its valid time), however this requires a more detailed investigation that is outside the scope of this paper.

Figure 12 shows the area averaged surface temperature increments in the ocean from the uncoupled and

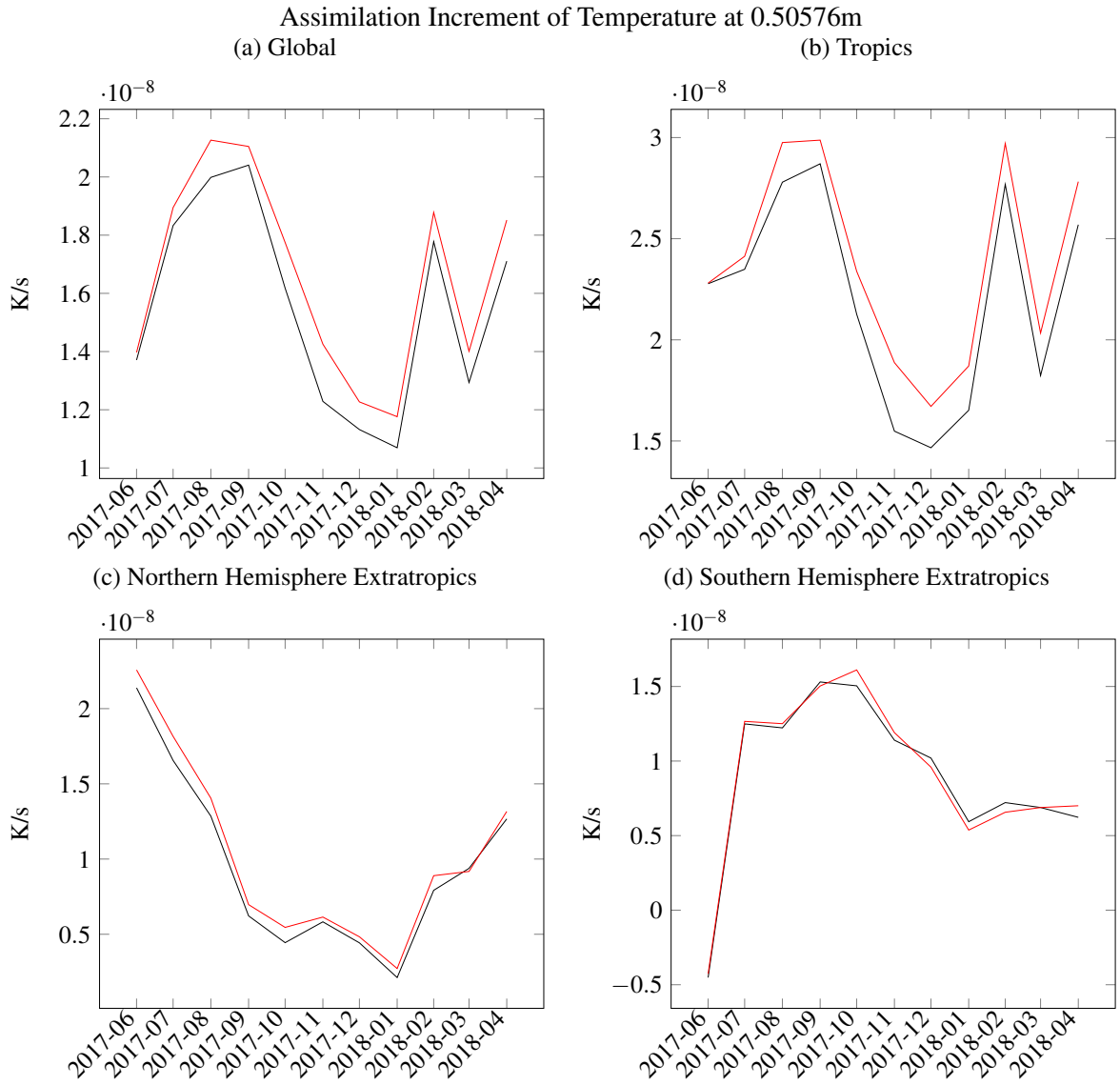

Figure 12: As Figure 11 but for surface assimilation temperature increments.

weakly coupled assimilation experiments. Similarly to Figure 11, the larger benefits from WCDA appear to be seen in the tropics with the coupling of SST, showing reduced increments compared to the uncoupled analysis. However in the northern hemisphere extratropics the weakly coupled assimilation increments are consistently smaller than the increments in the uncoupled system. For the southern hemisphere extratropics the picture is mixed and it seems like the 2 systems are behaving very similarly.

Operational impacts - Baltic sea detailed sea ice investigation

Here we take a detailed look at the spatial distribution of sea ice in the Baltic sea, a particularly challenging area for sea ice concentration analyses. Figure 13 shows different representations of the sea ice on 2018-02-17 from different sources. Figure 13a is a manually produced ice chart from FMI/SMHI showing sea ice concentration at the north of the Gulf of Bothnia, as well as in the eastern end of the Gulf of Finland. Figure 13b shows the available OSI SAF L3 sea ice concentration observations in the area. Note that because of the geography of the area observations are only available in the centre of the Gulfs - coastal contamination requires that those points near the coast be masked from the product.

Figures 13c and 13d show the sea ice from uncoupled assimilation and WCDA experiments. One can see that the uncoupled analysis effectively smooths out the L3 observations and does not capture the high ice concentrations along the northern coastlines. WCDA on the other hand does a much better job at capturing the structures seen in the manual ice chart. In particular the use of the background information coming from the dynamical model gives a much more realistic spatial distribution of the ice field. Figure 14 is similar but on 2018-03-05, the date of maximal sea ice extent in the Baltic sea for the 2017/2018 season.

5 Conclusions and future plans

This paper has investigated the impact of weakly coupled ocean–atmosphere data assimilation on the ECMWF forecasts. The WCDA approach allows components of the Earth system with different timescales and assimilation methods to be linked together. As an alternative to using purely observation based L4 products for the lower boundary of the atmosphere, with their associated latencies, WCDA allows dynamical models of the ocean and sea ice to fill in the gaps in observations and propagate fields to the appropriate time. The results presented show the use of WCDA improves the coupled forecasts in the regions near to the interface of those variables being coupled.

ECMWF's operational upgrade to cycle 45R1 in June 2018 saw the introduction of WCDA through sea ice concentration. The forthcoming upgrade to cycle 46R1 is scheduled to also couple tropical SST, as per the experiments shown in this paper.

As well as surface temperature and ice concentration information, the ocean analysis system can provide surface current information. Surface currents can be important for the assimilation of scatterometer data. Scatterometers measure backscattering coefficient of the ocean surface. This coefficient is a function of wind velocity relative to the ocean current. In the current usage of scatterometers at ECMWF we assume zero ocean currents, and so a WCDA system that has knowledge of the ocean currents should be able to better make use of scatterometer data.

There is plenty of scope to improve the partial coupling approach and its geospatial structure that determines the extent of SST coupling in the WCDA system. At the moment it is a simple function of latitude. It may be beneficial for this to be basin dependent. Given the model biases in the western boundary currents it may be beneficial to be different in the west and east of each basin.

These are the first steps in operational coupled ocean–atmosphere assimilation at ECMWF. A progressive approach towards implementation has been adopted, rather than introducing coupling in all variables in a single system upgrade. Whilst the weakly coupled approach is being developed, in parallel the outer loop coupling approach is being explored as a possible operational system which would give more immediate impact across the various Earth system components.

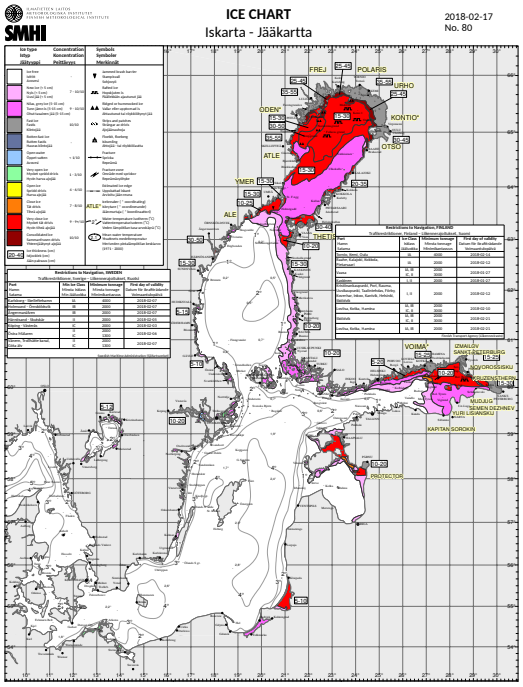

(a) Manually produced Finnish-Swedish Ice Chart of the Baltic Sea. © FMI and SMHI [2018] Reproduced with permission.

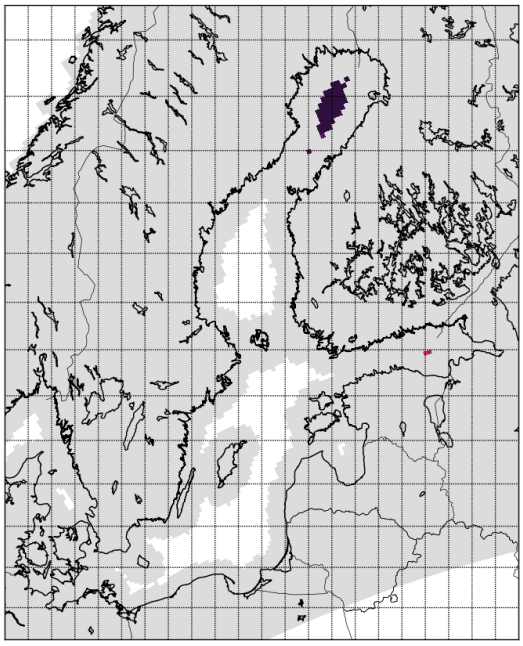

(b) OSI SAF 401-b product. Note missing data (grey) around coastlines due to coastal contamination in satellite retrievals of sea ice concentration.

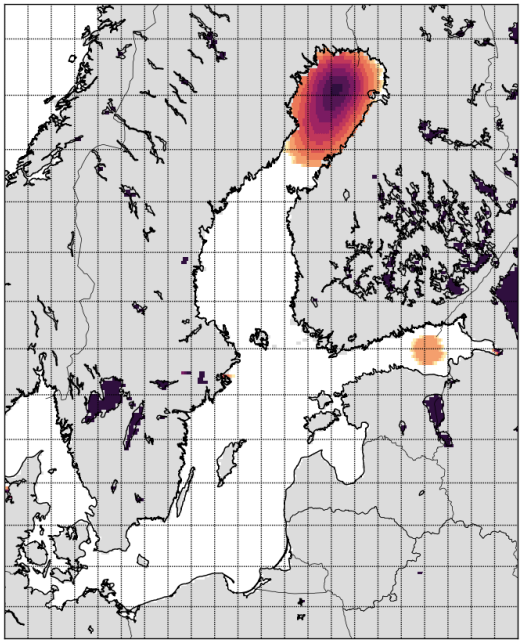

(c) Uncoupled analysis. Note the Gaussian nature of the ice field centred on the available OSI SAF L3 observations.

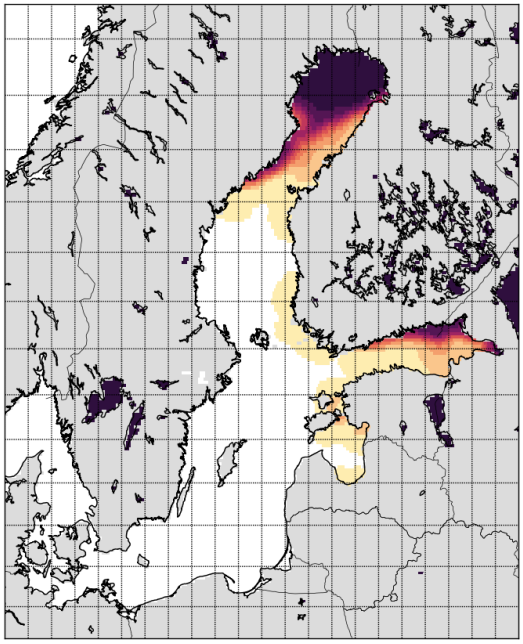

(d) WCDA. Note the much more realistic structure and the good agreement with the manual ice chart.

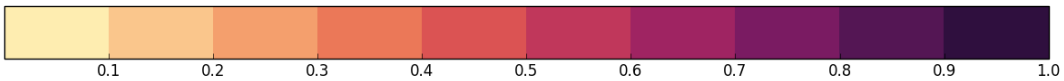

Figure 13: A manual ice chart (top left) and sea ice concentration values in the Baltic sea on 2018-02-17 from OSI SAF L3 observations (top right), uncoupled analysis (bottom left), and WCDA (bottom right).

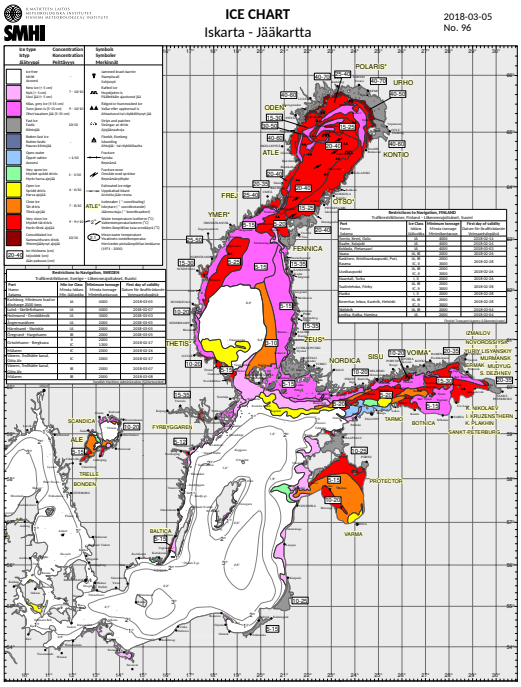

(a) Manually produced Finnish-Swedish Ice Chart of the Baltic Sea. © FMI and SMHI [2018] Reproduced with permission.

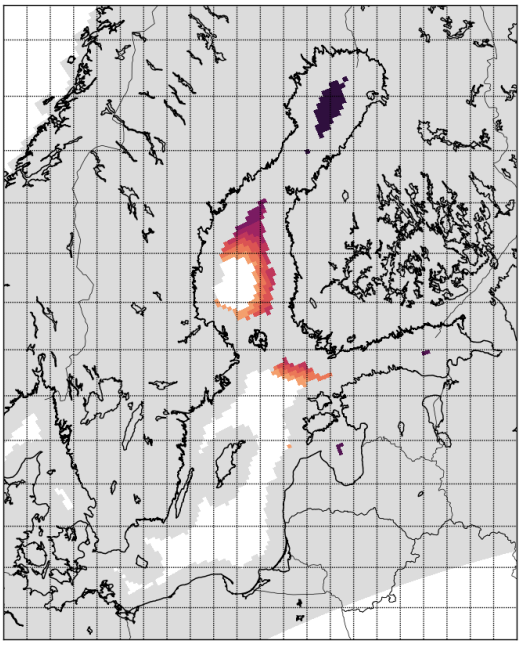

(b) OSI SAF 401-b product. Note missing data (grey) around coastlines due to coastal contamination in satellite retrievals of sea ice concentration.

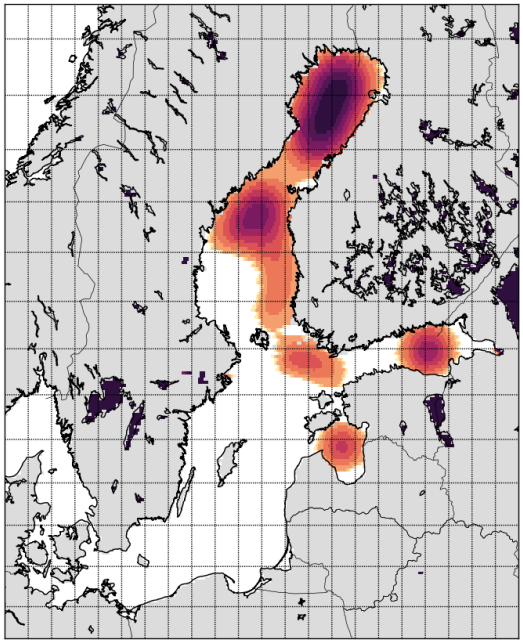

(c) Uncoupled analysis. Note the Gaussian nature of the ice field centred on the available OSI SAF L3 observations.

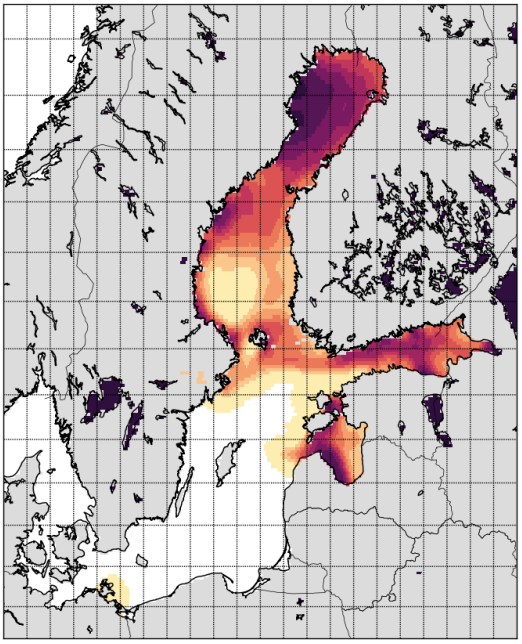

(d) WCDA. Note the much more realistic structure and the good agreement with the manual ice chart.

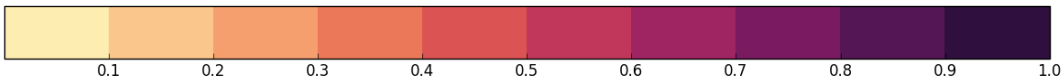

Figure 14: As Figure 13, but on 2018-03-05, the date of maximum sea ice extent in the region for the season.

6 Acknowledgements

We are grateful to Patrick Eriksson of FMI for providing assistance with the FMI/SMHI sea ice charts. Our thanks go to Magdalena Balmaseda, Stephen English, Sarah Keeley, and Kristian Mogensen for their help with implementations and insightful discussion of results.

References

M. A. Balmaseda, K. Mogensen, and A. T. Weaver. Evaluation of the ECMWF ocean reanalysis system ORAS4. *Quarterly Journal of the Royal Meteorological Society*, 139(674):1132–1161, 2013. ISSN 00359009. doi: 10.1002/qj.2063.

G. Balsamo, A. Beljaars, K. Scipal, P. Viterbo, B. van den Hurk, M. Hirschi, and A. K. Betts. A Revised Hydrology for the ECMWF Model: Verification from Field Site to Terrestrial Water Storage and Impact in the Integrated Forecast System. *Journal of Hydrometeorology*, 10(3):623–643, 2009. ISSN 1525-755X. doi: 10.1175/2008JHM1068.1. URL http://journals.ametsoc.org/doi/abs/10.1175/2008JHM1068.1.

P. Bauer and D. Richardson. New model cycle 40r1. *ECMWF Newsletter No. 138 - Winter 2013/2014*, (138):3, 2014. URL www.ecmwf.int/publications/newsletter.

P. Bauer, A. Thorpe, and G. Brunet. The quiet revolution of numerical weather prediction. *Nature*, 525 (7567):47–55, 2015. ISSN 0028-0836. doi: 10.1038/nature14956. URL http://www.nature.com/doifinder/10.1038/nature14956.

M. Bonavita, L. Isaksen, and E. Hólm. On the use of EDA background error variances in the ECMWF 4D-Var. *Quarterly Journal of the Royal Meteorological Society*, 138(667):1540–1559, jul 2012. ISSN 00359009. doi: 10.1002/qj.1899. URL http://doi.wiley.com/10.1002/qj.1899.

P. de Rosnay, G. Balsamo, C. Albergel, J. Muñoz-Sabater, and L. Isaksen. Initialisation of Land Surface Variables for Numerical Weather Prediction. *Surveys in Geophysics*, 35(3):607–621, 2014. ISSN 01693298. doi: 10.1007/s10712-012-9207-x.

C. J. Donlon, M. Martin, J. Stark, J. Roberts-Jones, E. Fiedler, and W. Wimmer. The Operational Sea Surface Temperature and Sea Ice Analysis (OSTIA) system. *Remote Sensing of Environment*, 116: 140–158, jan 2012. ISSN 00344257. doi: 10.1016/j.rse.2010.10.017. URL http://linkinghub.elsevier.com/retrieve/pii/S0034425711002197.

E. Dutra, V. M. Stepanenko, G. Balsamo, P. Viterbo, P. M. A. Miranda, D. Mironov, and C. Schär. Impact of lakes on the ECMWF surface scheme. *ECMWF Technical Memorandum*, (November 2009):1–15, 2009.

ECMWF. *PART V: ENSEMBLE PREDICTION SYSTEM*. Number 5 in IFS Documentation. ECMWF, 2014.

ECMWF. The Strength of a Common Goal: A Roadmap To 2025. Technical report, ECMWF, 2016. URL https://www.ecmwf.int/sites/default/files/ECMWF{_}Roadmap{_}to{_}2025.pdf.

ECMWF. *PART III: DYNAMICS AND NUMERICAL PROCEDURES*. Number 3 in IFS Documentation. ECMWF, 2017a.

ECMWF. *PART IV: PHYSICAL PROCESSES*. Number 4 in IFS Documentation. ECMWF, 2017b.

ECMWF. *PART VII: ECMWF WAVE MODEL*. Number 7 in IFS Documentation. ECMWF, 2017c.

S. English, A. McNally, N. Borman, K. Salonen, M. Matricardi, A. Horányi, M. Rennie, M. Janisková, S. Di Michele, A. Geer, E. Di Tomaso, C. Cardinali, P. de Rosnay, J. Sabater, M. Bonavita, C. Albergel, R. Engelen, and J.-N. Thépaut. Impact of Satellite Data. *Technical Memoradum ECMWF*, (711):46, 2013.

FMI and SMHI. Baltic sea ice chart, 2018. URL http://cdn.fmi.fi/marine-observations/products/ice-charts/20180217-full-color-ice-chart.pdf.

S. Frolov, C. H. Bishop, T. Holt, J. Cummings, and D. Kuhl. Facilitating Strongly Coupled OceanAtmosphere Data Assimilation with an Interface Solver. *Monthly Weather Review*, 144(1):3–20, 2016. ISSN 0027-0644. doi: 10.1175/MWR-D-15-0041.1. URL http://journals.ametsoc.org/doi/abs/10.1175/MWR-D-15-0041.1.

A. J. Geer. Significance of changes in medium-range forecast scores. *Tellus A*, 68(0):1–21, 2016. ISSN 1600-0870. doi: 10.3402/tellusa.v68.30229. URL http://www.tellusa.net/index.php/tellusa/article/view/30229.

T. Haiden, M. Dahoui, B. Ingleby, P. D. Rosnay, C. Prates, E. Kuscu, T. Hewson, L. Isaksen, D. Richardson, H. Zuo, and L. Jones. Use of in situ surface observations at ECMWF. *Technical Memoradum ECMWF*, 834(November), 2018.

J. Haseler. The early-delivery suite. Technical memorandum 454, ECMWF, 2004.

S. Keeley et al. The ECMWF Coupled Atmosphere-Wave-Ocean-Ice Model as Implemented in CY45R1: Part 3: Ice model performance. *ECMWF Technical Memorandum*, 2019.

P. Laloyaux, M. Balmaseda, D. Dee, K. Mogensen, and P. Janssen. A coupled data assimilation system for climate reanalysis. *Quarterly Journal of the Royal Meteorological Society*, 142(694):65–78, 2016. ISSN 1477870X. doi: 10.1002/qj.2629.

D. J. Lea, I. Mirouze, M. J. Martin, R. R. King, A. Hines, D. Walters, and M. Thurlow. Assessing a New Coupled Data Assimilation System Based on the Met Office Coupled Atmosphere-LandOceanSea Ice Model. *Monthly Weather Review*, 143(11):4678–4694, 2015. ISSN 0027-0644. doi: 10.1175/MWR-D-15-0174.1. URL http://journals.ametsoc.org/doi/10.1175/MWR-D-15-0174.1.

C. Maclachlan, A. Arribas, K. A. Peterson, A. Maidens, D. Fereday, A. A. Scaife, M. Gordon, M. Vellinga, A. Williams, R. E. Comer, J. Camp, P. Xavier, and G. Madec. Global Seasonal forecast system version 5 (GloSea5): A high-resolution seasonal forecast system. *Quarterly Journal of the Royal Meteorological Society*, 141(689):1072–1084, 2015. ISSN 1477870X. doi: 10.1002/qj.2396.

S. Masuda, J. Philip Matthews, Y. Ishikawa, T. Mochizuki, Y. Tanaka, and T. Awaji. A new Approach to El Niño Prediction beyond the Spring Season. *Scientific Reports*, 5:1–9, 2015. ISSN 20452322. doi: 10.1038/srep16782.

T. Mochizuki, S. Masuda, Y. Ishikawa, and T. Awaji. Multiyear climate prediction with initialization based on 4D-Var data assimilation. *Geophysical Research Letters*, 43(8):3903–3910, 2016. ISSN 19448007. doi: 10.1002/2016GL067895.

K. Mogensen et al. The ECMWF Coupled Atmosphere-Wave-Ocean-Ice Model as Implemented in CY45R1: Part 1: technical implementation. *ECMWF Technical Memorandum*, 2019a.

K. Mogensen et al. The ECMWF Coupled Atmosphere-Wave-Ocean-Ice Model as Implemented in CY45R1: Part 2: Ocean model performance. *ECMWF Technical Memorandum*, 2019b.

D. P. Mulholland, P. Laloyaux, K. Haines, and M. Alonso Balmaseda. Origin and Impact of Initialization Shocks in Coupled Atmosphere-Ocean Forecasts. *Monthly Weather Review*, 143:4631–4644, 2015. ISSN 0027-0644. doi: 10.1175/MWR-D-15-0076.1. URL https://www.ecmwf.int/sites/default/files/ECMWF{_}Roadmap{_}to{_}2025.pdf.

S. G. Penny, S. Akella, O. Alves, C. Bishop, M. Buehner, M. Chevallier, F. Counillon, C. Draper, S. Frolov, Y. Fujii, A. Karspeck, A. Kumar, P. Laloyaux, J.-F. Mahfouf, M. Martin, M. Pena, P. De Rosnay, A. Subramanian, R. Tardif, Y. Wang, and X. Wu. Coupled Data Assimilation for Integrated Earth System Analysis and Prediction: Goals, Challenges and Recommendations. Technical report, World Meteorological Organisation, 2017.

F. Rabier, H. Järvinen, E. Klinker, J.-F. Mahfouf, and A. Simmons. The ECMWF operational implementation of four-dimensional variational assimilation. Part I: Experimental results and diagnostics wiht operational configuration. *Q. J. R. Meteorol. Soc.*, 126:1143–1170, 2000. ISSN 1477-870X. doi: 10.1002/qj.49712656417.

S. Saha, S. Moorthi, H. L. Pan, X. Wu, J. Wang, S. Nadiga, P. Tripp, R. Kistler, J. Woollen, D. Behringer, H. Liu, D. Stokes, R. Grumbine, G. Gayno, J. Wang, Y. T. Hou, H. Y. Chuang, H. M. H. Juang, J. Sela, M. Iredell, R. Treadon, D. Kleist, P. Van Delst, D. Keyser, J. Derber, M. Ek, J. Meng, H. Wei, R. Yang, S. Lord, H. Van Den Dool, A. Kumar, W. Wang, C. Long, M. Chelliah, Y. Xue, B. Huang, J. K. Schemm, W. Ebisuzaki, R. Lin, P. Xie, M. Chen, S. Zhou, W. Higgins, C. Z. Zou, Q. Liu, Y. Chen, Y. Han, L. Cucurull, R. W. Reynolds, G. Rutledge, and M. Goldberg. The NCEP climate forecast system reanalysis. *Bulletin of the American Meteorological Society*, 91(8):1015–1057, 2010. ISSN 00030007. doi: 10.1175/2010BAMS3001.1.

S. Saha, S. Moorthi, X. Wu, J. Wang, S. Nadiga, P. Tripp, D. Behringer, Y. T. Hou, H. Y. Chuang, M. Iredell, M. Ek, J. Meng, R. Yang, M. P. Mendez, H. Van Den Dool, Q. Zhang, W. Wang, M. Chen, and E. Becker. The NCEP climate forecast system version 2. *Journal of Climate*, 27(6):2185–2208, 2014. ISSN 08948755. doi: 10.1175/JCLI-D-12-00823.1.

D. Schepers, E. D. Boisséson, R. Eresmaa, C. Lupu, and P. D. Rosnay. CERA-SAT: A coupled satellite-era reanalysis. *ECMWF Newsletter*, (155):32–37, 2018. doi: 10.21957/sp619ds74g.

T. N. Stockdale, D. L. Anderson, J. O. Alves, and M. A. Balmaseda. Global seasonal rainfall forecasts using a coupled ocean-atmosphere model. *Nature*, 392(6674):370–373, 1998. ISSN 00280836. doi: 10.1038/32861.

N. Sugiura, T. Awaji, S. Masuda, T. Mochizuki, T. Toyoda, T. Miyama, H. Igarashi, and Y. Ishikawa. Development of a four-dimensional variational coupled data assimilation system for enhanced analysis and prediction of seasonal to interannual climate variations. *Journal of Geophysical Research: Oceans*, 113(10):1–21, 2008. ISSN 21699291. doi: 10.1029/2008JC004741.

F. Vitart. Monthly Forecasting at ECMWF. *Mon. Wea. Rev.*, 132(1986):2761–2779, 2004. ISSN 0027-0644. doi: 10.1175/MWR2826.1.

X. Yang, A. Rosati, S. Zhang, T. L. Delworth, R. G. Gudgel, R. Zhang, G. Vecchi, W. Anderson, Y. soon Chang, T. Delsole, K. Dixon, R. Msadek, W. F. Stern, A. Wittenberg, and F. Zeng. A predictable AMO-like pattern in the GFDL fully coupled ensemble initialization and decadal forecasting system. *Journal of Climate*, 26(2):650–661, 2013. ISSN 08948755. doi: 10.1175/JCLI-D-12-00231.1.

S. Zhang, Y. S. Chang, X. Yang, and A. Rosati. Balanced and coherent climate estimation by combining data with a biased coupled model. *Journal of Climate*, 27(3):1302–1314, 2014. ISSN 08948755. doi: 10.1175/JCLI-D-13-00260.1.

H. Zuo, M. A. Balmaseda, K. Mogensen, and S. Tietsche. OCEAN5: the ECMWF Ocean Reanalysis System and its Real-Time analysis component. Technical Report 823, ECMWF, 2018.

A Appendix: area averaged dRMSE of forecast errors

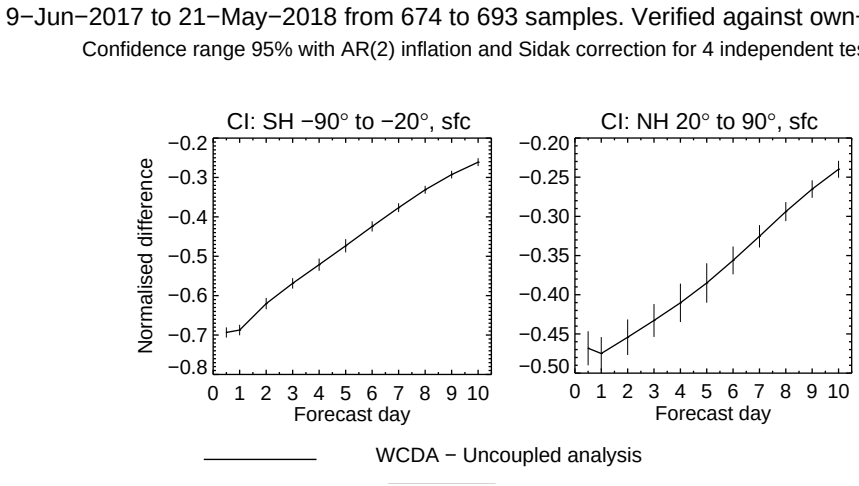

Figure 15: Area averaged diagram of the normalised difference in RMSE between WCDA and control for sea ice concentration in the southern hemisphere (left), tropics (centre) and northern hemisphere (right) for forecasts at lead times of up to 10 days.

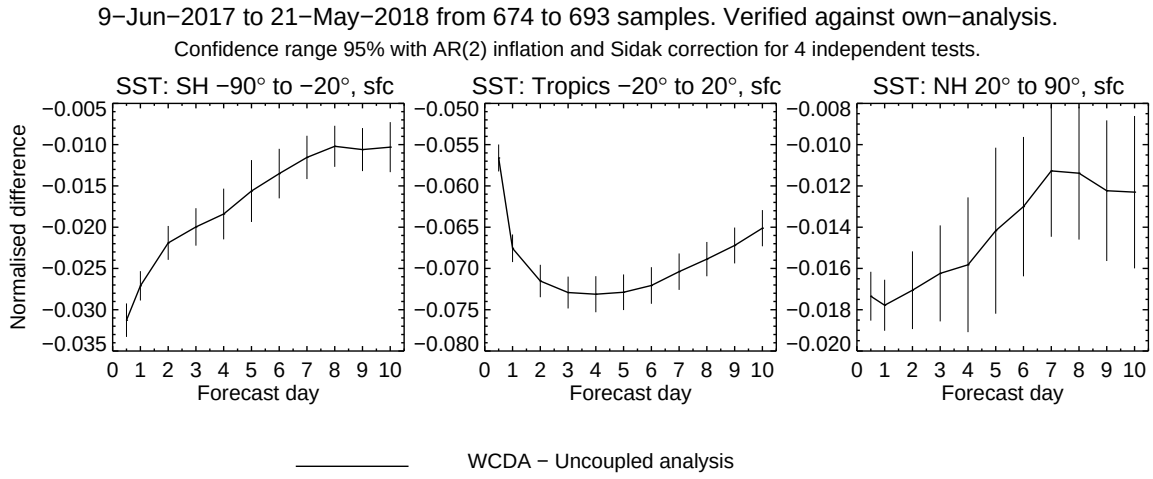

Figure 16: As Figure 15 but for sea-surface temperature.

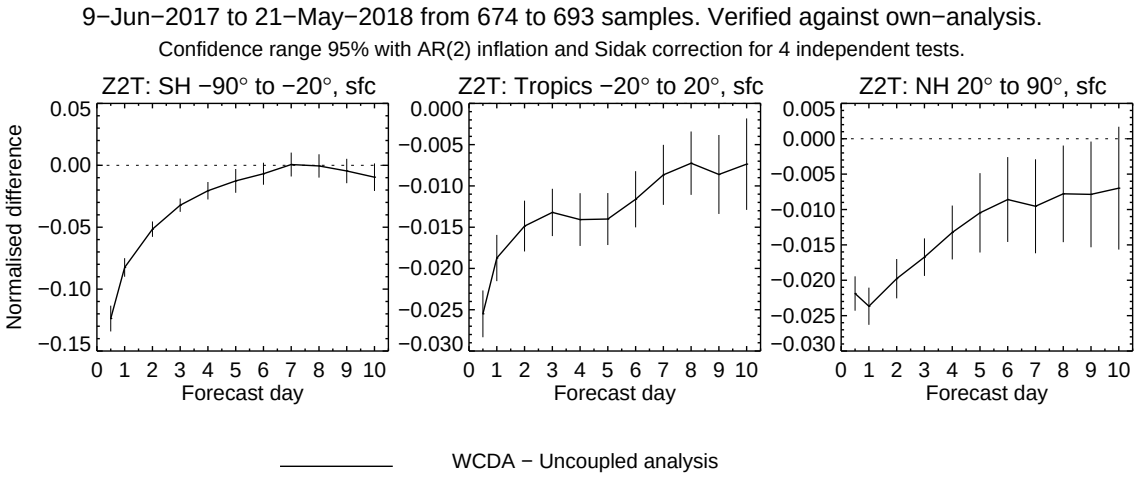

Figure 17: As figure 15 but for atmospheric 2 metre temperature.

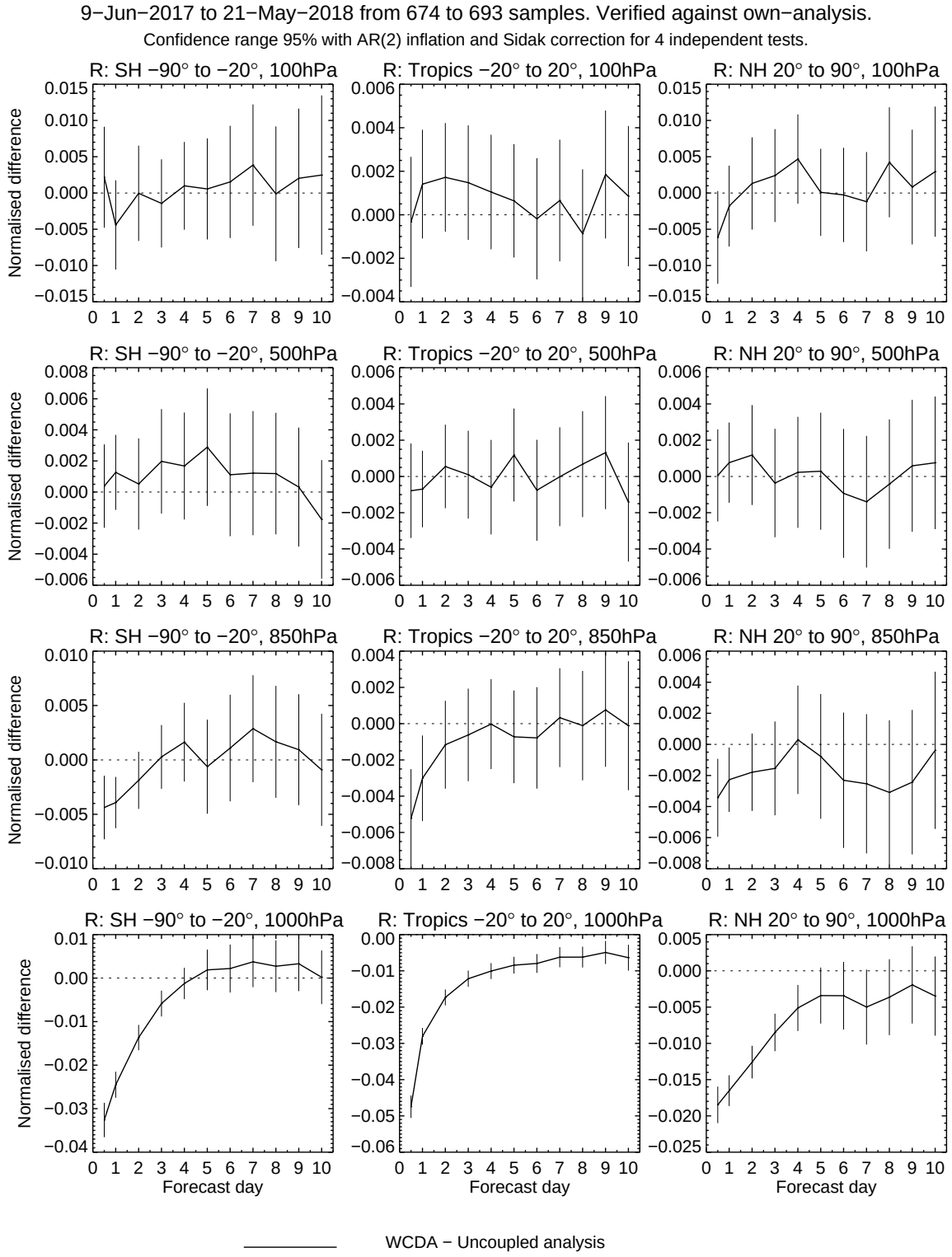

Figure 18: As Figure 15 but for atmospheric relative humidity and stratified by level, 100hPa (top row), 500hPa (second row), 850hPa (third row) and 1000hPa (bottom row).

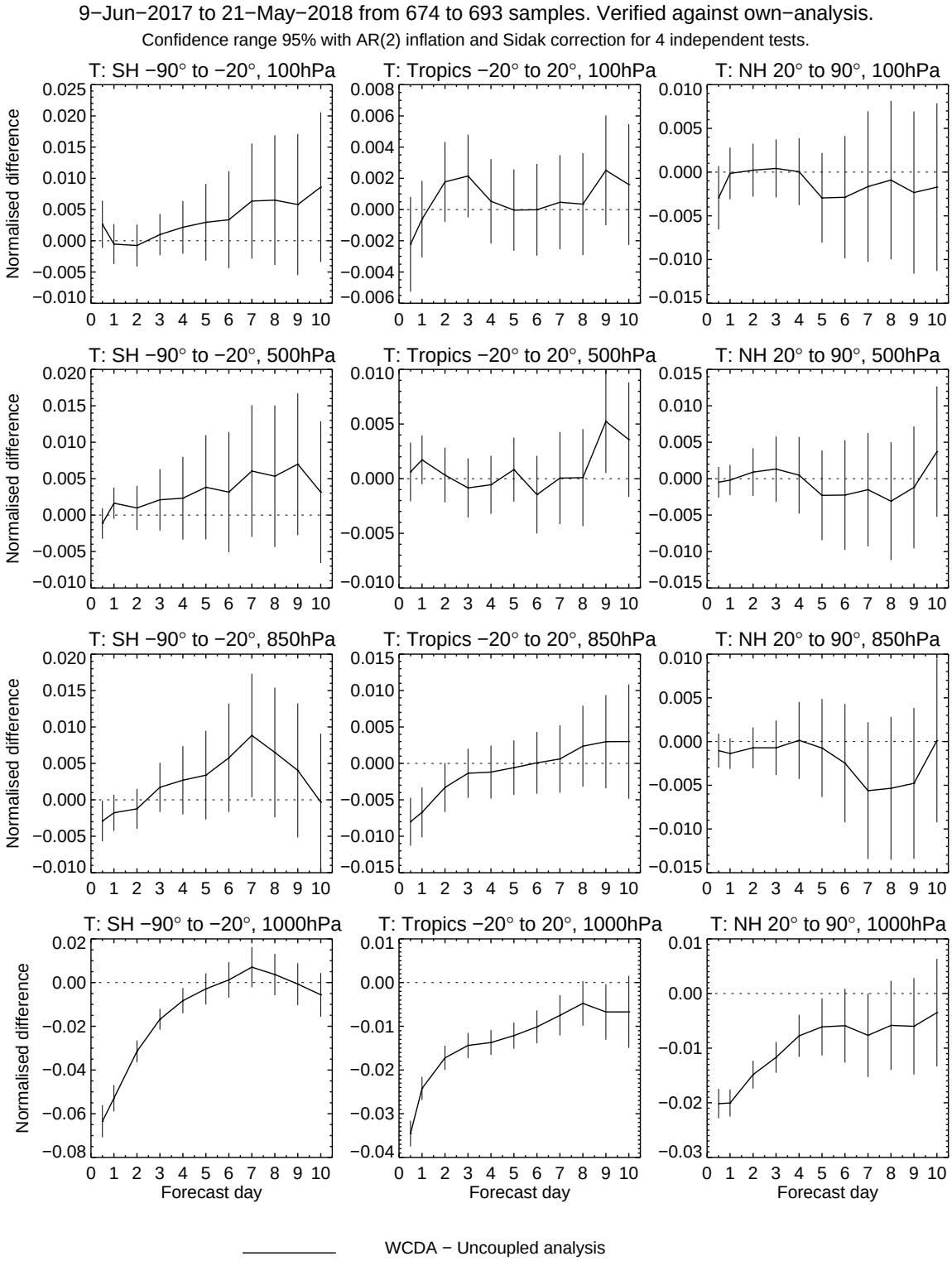

Figure 19: As Figure 18 but for atmospheric temperature.